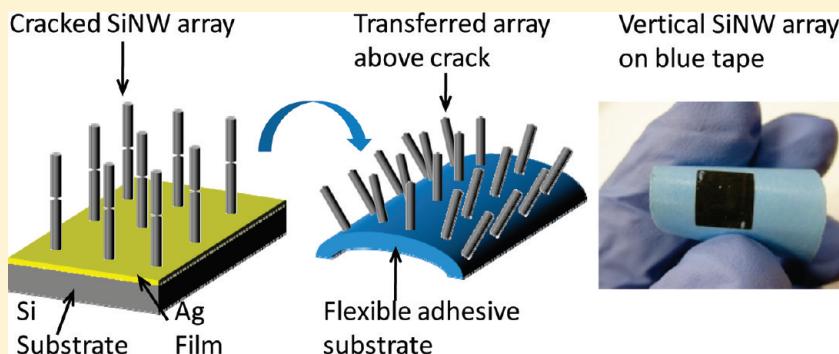


Vertical Transfer of Uniform Silicon Nanowire Arrays via Crack Formation

Jeffrey M. Weisse, Dong Rip Kim, Chi Hwan Lee, and Xiaolin Zheng*

Department of Mechanical Engineering, Stanford University, California 94305, United States

ABSTRACT:



Vertical transfer of silicon nanowire (SiNW) arrays with uniform length onto adhesive substrates was realized by the assistance of creating a horizontal crack throughout SiNWs. The crack is formed by adding a water soaking step between consecutive Ag-assisted electroless etching processes of Si. The crack formation is related to the delamination, redistribution, and reattachment of the Ag film during the water soaking and subsequent wet etching steps. Moreover, the crack facilitates embedding SiNWs inside polymers.

KEYWORDS: Nanowire transfer, silicon nanowire, crack formation, Ag etching, embedding nanowires

Uniform, vertically aligned silicon nanowire (SiNW) arrays are promising building blocks for a range of vertical devices, such as surround-gate field-effect transistors,^{1–3} solar cells,^{4,5} and thermoelectric modules.^{6–8} Although vertically aligned SiNW arrays can be fabricated with a relatively high degree of control and uniformity through both the top-down etching^{9–11} and the bottom-up epitaxial growth methods,^{12,13} these SiNW arrays are frequently attached in series to silicon wafers. Hence, it is a challenge to express and utilize the inherent electrical and optical properties of the SiNW arrays for devices because the SiNW array properties are typically overshadowed by the properties of the much thicker bulk silicon wafers. Efforts have been made to distinguish the electrical and optical properties of the SiNWs from that of the substrate while maintaining the vertical structure of SiNW arrays. One approach used a heavily doped Si wafer and a thin lightly doped Si layer was epitaxially grown on top in which the SiNWs were formed by etching.⁴ However, growing an epitaxial layer is a time-consuming, expensive process and this technique is only suitable for investigating lightly doped SiNW arrays. Another approach fabricated SiNW arrays on a silicon on insulator (SOI) wafer and used KOH to selectively remove the backside Si, and as such the optical properties of the SiNW arrays were characterized.¹⁴ It is more desirable to remove vertical NW arrays from their growth substrate and attach the removed NW arrays to a different substrate for vertical devices. One method embedded a Si wire array inside polydimethylsiloxane (PDMS),

which was further peeled off from the substrate, however this method has only been demonstrated for ultralong wires with large interwire spacing.¹⁵ The other approach cemented the SiNWs into a 290 nm thick poly(methyl methacrylate) (PMMA) layer and fractured the SiNWs from the silicon substrate by applying a shear force while maintaining their vertical alignment in the PMMA.¹⁶ Nevertheless, an extremely high insertion pressure of 55 kg/cm² was required to push the array into the PMMA, which resulted in the SiNW tips bundling within the PMMA and damage of the vertical alignment.¹⁶ More importantly, the SiNWs fracture at random locations, which causes the transferred SiNWs to have nonuniform lengths. Here, we report an alternative and yet simple method to chemically weaken a designated segment of vertically aligned SiNW arrays by using Ag-assisted electroless etching,¹⁷ which enables controlled transfer of uniform, vertically aligned SiNWs to foreign substrates with high quality.

Specifically, a well-controlled horizontal crack parallel to the wafer surface was formed over a large area through an array of vertically aligned SiNWs. The formation process of the crack is illustrated in Figure 1. The SiNW array was fabricated by the well-established Ag-assisted electroless wet etching technique.¹⁷

Received: December 14, 2010

Revised: January 26, 2011

Published: February 15, 2011

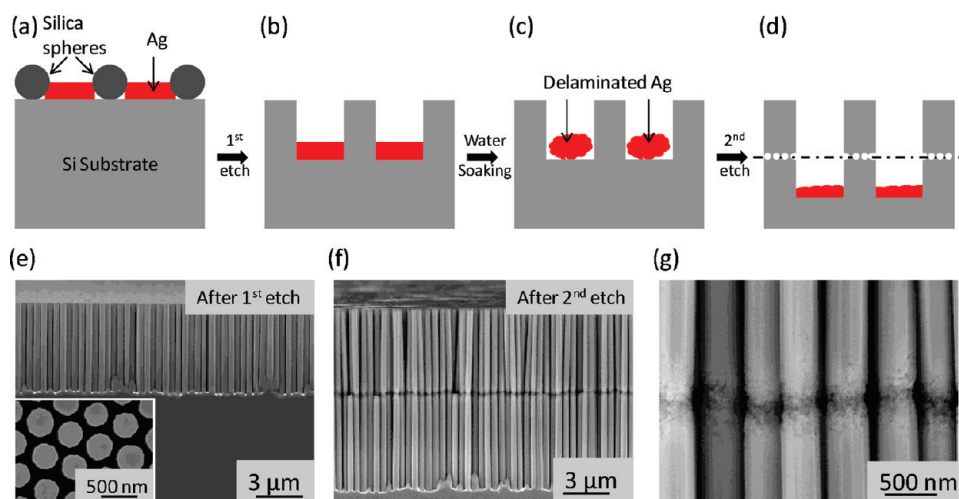


Figure 1. Schematic of the fabrication procedure for the cracked SiNW array. (a) Ag film is patterned by using silica spheres, (b) a SiNW array is formed after the first etch, (c) Ag is delaminated from Si after soaking the wafer in 75 °C DI water for 3 h, (d) a horizontal crack is formed after the second etch, along with the elongation of the SiNWs. SEM images of SiNWs (e) after the first etch, (f) after the second etch, and (g) with a zoom-in view of the crack.

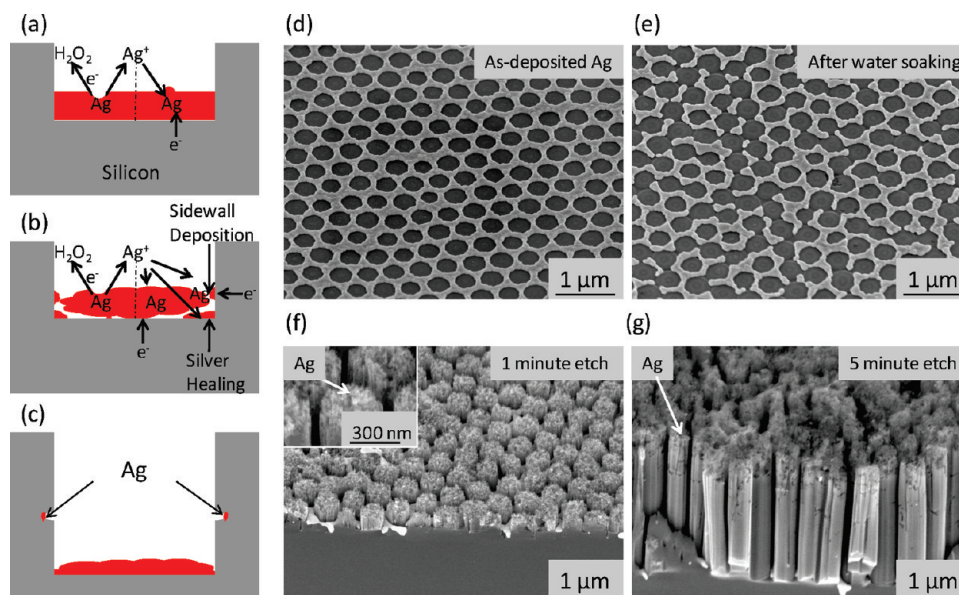
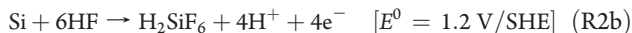
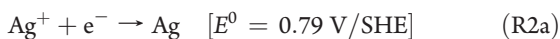
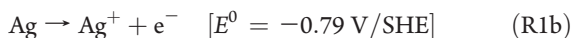


Figure 2. The crack formation mechanism. Schematic of (a) the reactions occurring at the etchant/Ag (left) and Ag/Si (right) interface when the Ag has good adhesion with Si, (b) when the Ag is delaminated from the Si, a surplus of Ag^+ ions is formed in the solution, leading to Ag particle deposition on the sidewalls of the SiNWs and on the Si wafer beneath the Ag film, (c) the delaminated Ag film is healed and reattached to the Si wafer while the SiNWs continue to elongate. SEM images of the patterned Ag film (d) as deposited, (e) after soaking in 75 °C DI water for 3 h, and subsequently etched in HF/ H_2O_2 mixture for (f) 1 min and (g) 5 min.

Silica (SiO_2) spheres were synthesized by a modified Stöber synthesis method,¹⁸ deposited as a monolayer on a Si(100) wafer via Langmuir–Blodgett assembly, etched by reactive ions to a desired diameter in a gas mixture of O_2 and CHF_3 ,¹⁹ and followed by e-beam evaporation of a 50 nm thick silver film. The SiO_2 spheres were then removed ultrasonically in isopropyl alcohol (IPA), resulting in a honeycomb-pattern silver film, as shown in Figure 1a.^{9,10,20} SiNWs were then formed by immersing the Si wafer in an etchant solution of 4.6 M hydrofluoric acid (HF) and 0.4 M hydrogen peroxide (H_2O_2),^{10,11,21} where directional etching of Si occurs along the [100] direction.^{22–24} Once the desired SiNW length was achieved by the timed etch, the wafer was rinsed in deionized (DI) water and dried by N_2 . Subsequently, the Si

wafer was soaked in a 75 °C DI water bath for about three hours, which delaminated the Ag film (Figures 1c and 2e).^{25,26} Afterward, the Si wafer was promptly dried by N_2 and immediately returned back into the etching solution. A horizontal crack was formed at the start of the second etch while the etching continued to elongate the SiNWs (Figure 1d). Scanning electron microscopy (SEM) images show that the vertically aligned SiNW array has a uniform length (about 5 μm) after the first etch (Figure 1e) and is separated into two uniform length layers of 5 μm each after the second etch (Figure 1f). A zoomed-in SEM image shows that the Si is partially etched away at the crack location of the SiNWs, which weakens the connection between the top and bottom SiNW array layers (Figure 1g).

The formation of the horizontal crack in the SiNWs is closely related to the delamination of the Ag film, and the electrochemical reactions during the etching process. The etching process of the SiNWs consists of two pairs of redox reactions: one occurs at the interface between the Ag film and the etching solution (R1) and the other occurs at the Ag/Si interface (R2).^{11,21,27}



At the Ag/etchant interface, Ag is oxidized by H_2O_2 (R1a and R1b), forming Ag^+ ions in the vicinity of the Ag film (Figure 2a).^{21,27,28} The formed Ag^+ ions are subsequently reduced back to Ag by R2a preferably onto the surface of Ag instead of Si, since Ag is more electronegative than Si.^{27,29,30} Meanwhile, the Si is oxidized by R2b and further dissolved by HF, resulting in the formation of SiNWs.^{27,29–31} Normally, when the Ag film has good contact with the Si, the production of the Ag^+ ions by R1 is balanced by the consumption of the Ag^+ ions by R2, so the Ag film remains mostly intact. However, when the Ag film is delaminated (Figure 2b), the Ag/etchant interfacial area is increased (Figure 2b), which speeds up the production rate of Ag^+ ions by R1. Meanwhile, the Ag/Si interfacial contact area is reduced, decreasing the amount of electrons transferred from Si to Ag, which consequently reduces the consumption rate of the Ag^+ ions by R2.²⁴ The combination of a faster R1 and a slower R2 results in a surplus of Ag^+ ions in the solution near the Ag film. This buildup of Ag^+ ions allows some of the Ag^+ ions to be reduced and deposited on the Si surface as new Ag particles, particularly in the proximity of the Ag film where the Ag^+ ion concentration is highest. The Ag particles deposited on the sidewalls of the SiNWs will etch horizontally through the SiNWs, leading to the formation of the crack (Figure 2b,c). Other Ag particles are deposited underneath the delaminated silver area, leading to the reattachment or “healing” of the Ag film to the Si wafer^{11,24} (Figure 2b,c). The healing process occurs quickly as the second etching step progresses, so the sidewalls of the SiNWs formed during the second etching become smooth again (Figures 1g and 2c). To confirm this effect, the as-deposited Ag film which has a well-defined pattern and good adhesion to the Si wafer (Figure 2d) was soaked in DI water for 3 h at 75 °C, and the Ag film clearly became delaminated afterward (Figure 2e). When we used this delaminated Ag film to etch SiNWs, the top and sidewalls of the SiNWs were very corrugated and some Ag particles could be found on top of and inside of the SiNWs throughout the sample after 1 min of etching (Figure 2f). However after 5 min of etching, the sidewalls of the SiNWs became much smoother (Figure 2g), indicating that the Ag film was healed. In addition, it can be seen in Figure 2g that some Ag particles on top of the SiNWs caused some channel formations inside the SiNWs.

Cracked SiNW arrays can be formed over a broad range of Si wafers, varying in both doping types and doping concentrations. As shown in Figure 3, cracked SiNW arrays were successfully formed with both lightly (Figure 3a,c) and heavily (Figure 3b,d) doped P- or N-type Si wafers. It should be noted that the heavily doped SiNWs appear to be somewhat etched during the water

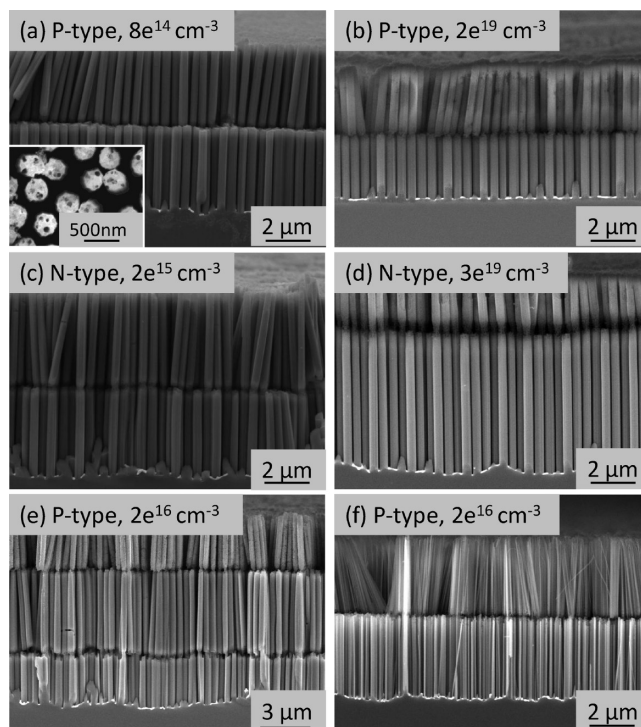


Figure 3. Generality of the crack formation. SEM images of cracked SiNWs fabricated using Si substrates that are (a) lightly doped P-type (inset, top view), (b) heavily doped P-type, (c) lightly doped N-type, and (d) heavily doped N-type. (e) SEM image of a SiNW array with two horizontal cracks. (f) SEM image of cracked SiNWs for which the Ag was deposited electrolessly in AgNO_3/HF .

soaking step, so their water soaking time was decreased to 30 min. Interestingly, as shown in Figure 3e, multiple cracks can be created at the desired axial locations along the SiNWs by adding multiple water-soaking steps between the time-controlled etching steps. In addition, the crack formation technique also applies to electrolessly deposited Ag.³² Figure 3f shows that a crack was also formed in a SiNW array fabricated by the steps outlined in Figure 1b–d, for which the Ag was electrolessly deposited by soaking the Si wafer in a 0.005 M AgNO_3 and 4.6 M HF solution for 1 min. Finally, it should be noted that the Ag^+ ion diffusion is not entirely localized, which roughens the surface of SiNWs above the crack, as shown in Figure 3b,e. Rough surfaces increase the scattering of electrons and phonons in SiNWs, which will reduce the thermal conductivity and the electron mobility. The surface roughness of SiNWs, when undesired, can be reduced by an oxidation process followed by a wet etching step to remove the surface oxide.^{33,34}

Creation of a horizontal crack through SiNW arrays enables the controlled breakage of the SiNWs at specified locations and facilitates their transfer to other substrates. Vertical transfer of the cracked SiNWs is achieved simply by attaching an adhesive surface to the top of the SiNW array and peeling off the adhesive receiver substrate, which fractures the NWs at the crack. The left column of Figure 4a demonstrates an example of using a thin spin-coated PMMA film as an adhesive on a receiver substrate.¹⁶ A cracked SiNW array was inserted into the PMMA by hand. The PMMA was then cured on a hot plate at 210 °C, which is above the glass transition temperature of the PMMA. This curing step cemented the SiNWs to the receiver substrate. Upon cooling, the Si substrate was easily removed by fracturing the SiNWs at the

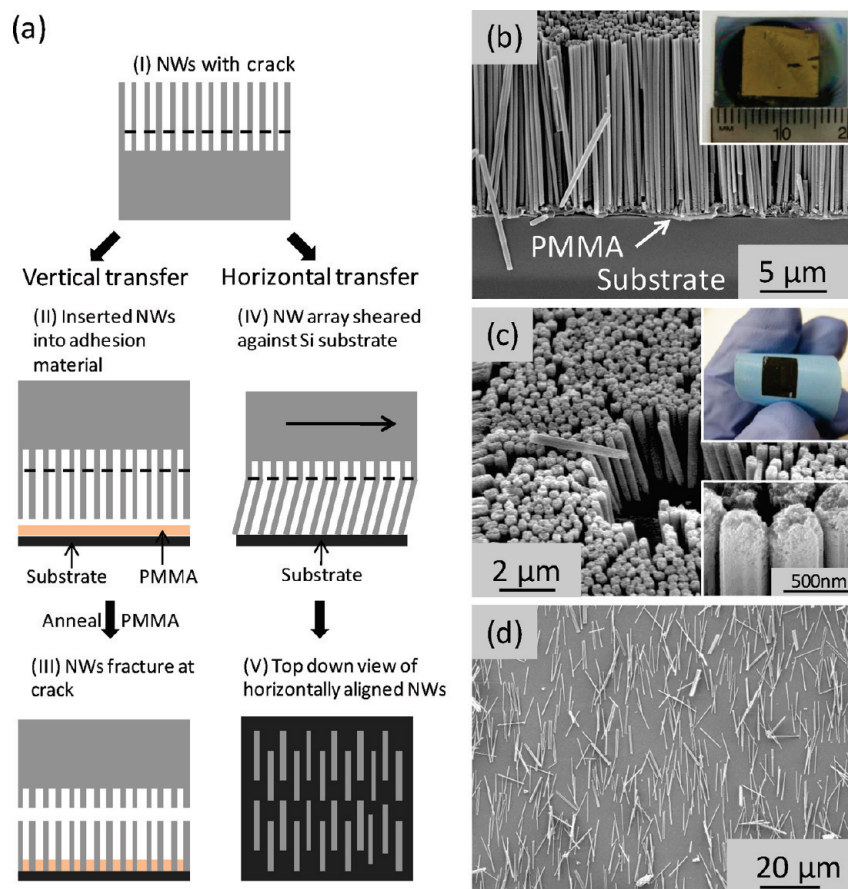


Figure 4. Transfer of the cracked SiNWs. (a) Schematic of vertical and horizontal transfers of the cracked SiNWs to foreign substrates. (Left column) Vertical transfer of SiNWs by inserting the cracked SiNW array into PMMA, followed by curing of the PMMA, and fracturing of the SiNWs. (Right column) Horizontal transfer of SiNWs by applying a shear force on the cracked SiNWs over a receiver substrate. SEM and optical (inset) images of (b) the vertical NWs transferred to a Si wafer coated with PMMA, (c) the vertical SiNW array on a blue tape and a zoomed-in view (lower inset) of the rough tips of NWs, and (d) the horizontal NWs with uniform length on a Si wafer.

crack, resulting in the transfer of vertically aligned, uniform length SiNWs to the receiver substrate over a relatively large area as shown in Figure 4b. Although a similar PMMA-assisted vertical transfer method has been demonstrated before,¹⁶ the presence of the crack greatly facilitates the separation of SiNWs from the donor Si wafer and improves the homogeneity of the transferred SiNW array. Furthermore, the cracked SiNWs can be easily peeled off from their fabrication substrate with adhesive tape, enabling the vertical transfer of SiNW arrays to flexible substrates. For example, Figure 4c shows that a SiNW array was transferred to blue tape over a large area with a high degree of vertical alignment. Finally, horizontal transfer of SiNWs to receiver substrates can be realized by the dry transfer method.³⁵ The SiNWs easily fracture at the crack during the transfer process, resulting in uniform length SiNWs depositing on the substrate with some degree of alignment (Figure 4d), which is important for reducing variations in the performance of NW-based devices. Although fractured SiNWs of uniform length have been demonstrated by using a “knocking-down” approach with an elastomer-covered rigid-roller, this method only applies to pattern planar NW devices on their growth substrate.³⁶ Our transfer methods with the presence of a crack through the SiNW array greatly facilitate the removal of uniform length SiNWs from their original substrates with the option of maintaining their vertical alignment. The transfer methods presented above

demonstrate that the presence of a crack through the SiNW array greatly facilitates the removal of uniform length SiNWs from their fabrication substrates.

In addition, the formation of the cracked SiNW array enables two other functionalities, that is, embedding the SiNWs within PDMS and integrating the SiNWs into channels. Embedding NWs within a polymer is needed to provide mechanical support and electrical and thermal insulations for NW-based flexible displays and energy-harvesting devices.^{37,38} This is typically realized by spin-coating hexane-diluted PDMS^{15,39} for which the spinning speed, duration, and the dilution of the PDMS need to be varied for NW arrays of different densities and dimensions. For our cracked SiNWs, we simply pour liquid PDMS into a precracked SiNW array. Upon degassing and curing, the PDMS can be peeled off along the cracked interface, forming a receiver and a donor substrate (Figure 5a). The receiver substrate (Figure 5c) is a flexible piece of PDMS with vertically aligned SiNWs embedded in one side. The donor substrate (Figure 5d) consists of the bottom SiNW layer embedded in the PDMS for which a metal contact can be easily deposited on top to form vertical SiNW devices. This is a simpler and more uniform technique to create polymer-filled SiNW arrays over a large area compared to the spin-coating method.³⁸ The other opportunity facilitated by the crack is the formation of a silicon trench with vertically aligned NWs at the bottom, which can increase the

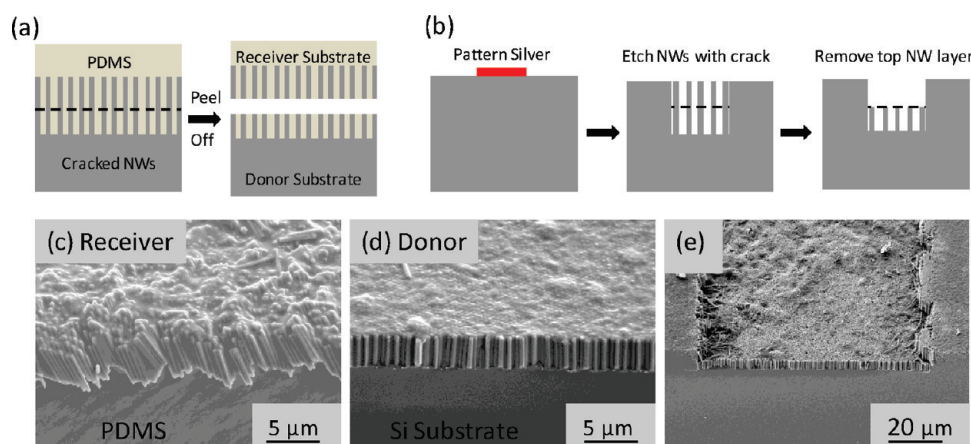


Figure 5. (a) Schematic of embedding vertically aligned SiNWs in PDMS, SEM images of (c) the corresponding receiver and (d) the donor substrates after peeling off the PDMS. (b) Schematic and (e) SEM image of the fabricated vertical SiNWs along the base of a trench.

surface area or promote mixing of a microfluidic channel without generating a significant pressure drop.¹² As shown in Figure 5b, the trench is formed by patterning the Ag film at selected areas, forming a cracked SiNW array, and removing the top SiNW layer with an adhesive material, such as tape. The SEM image in Figure 5e shows that uniform SiNWs are formed at the floor of the Si trench.

In summary, we present a simple water soaking technique to form horizontal cracks through Ag-assisted top-down SiNWs. The formation of the crack is caused by the delamination of the Ag film during the water soaking step and redistribution and reattachment of the Ag film during the subsequent wet etching step. Some of the Ag is redistributed as particles to the sidewalls of SiNWs close to the Ag film, which leads to a localized horizontal etch of the SiNWs forming the crack. Single or multiple cracks can be formed over various Si wafers with different doping types and doping concentrations. Furthermore, the crack enables the breakage of SiNWs with uniform lengths and greatly facilitates the vertical transfer of uniform SiNW arrays to other adhesive substrates, such as tapes and PMMA-coated substrates. In addition, the crack enables embedding the SiNWs within PDMS and integrating the SiNWs into channels. We believe that all the functionalities enabled by the crack may help facilitate the realization of vertical NW devices.

AUTHOR INFORMATION

Corresponding Author

*E-mail: xlzheng@stanford.edu.

ACKNOWLEDGMENT

This work is supported by NSF under award Number 0826003. D.R.K acknowledges support from the Link Foundation Energy Fellowship. The authors also thank Yunzhe Feng and Pratrapp M. Rao for discussions and Young-Beom Kim for silica sphere synthesis assistance.

REFERENCES

- (1) Goldberger, J.; Hochbaum, A. I.; Fan, R.; Yang, P. D. *Nano Lett.* **2006**, *6* (5), 973–977.
- (2) Lugstein, A.; Steinmair, M.; Henkel, C.; Bertagnolli, E. *Nano Lett.* **2009**, *9* (5), 1830–1834.

- (3) Manandhar, P.; Akhadov, E. A.; Tracy, C.; Picraux, S. T. *Nano Lett.* **2010**, *10* (6), 2126–2132.
- (4) Garnett, E.; Yang, P. D. *Nano Lett.* **2010**, *10* (3), 1082–1087.
- (5) Kelzenberg, M. D.; Boettcher, S. W.; Petykiewicz, J. A.; Turner-Evans, D. B.; Putnam, M. C.; Warren, E. L.; Spurgeon, J. M.; Briggs, R. M.; Lewis, N. S.; Atwater, H. A. *Nat. Mater.* **2010**, *9* (3), 239–244.
- (6) Abramson, A. R.; Kim, W. C.; Huxtable, S. T.; Yan, H. Q.; Wu, Y. Y.; Majumdar, A.; Tien, C. L.; Yang, P. D. *J. Microelectromech. Syst.* **2004**, *13* (3), 505–513.
- (7) Boukai, A. I.; Bunimovich, Y.; Tahir-Kheli, J.; Yu, J. K.; Goddard, W. A.; Heath, J. R. *Nature* **2008**, *451* (7175), 168–171.
- (8) Hochbaum, A. I.; Chen, R. K.; Delgado, R. D.; Liang, W. J.; Garnett, E. C.; Najarian, M.; Majumdar, A.; Yang, P. D. *Nature* **2008**, *451* (7175), 163–167.
- (9) Huang, Z. P.; Fang, H.; Zhu, J. *Adv. Mater.* **2007**, *19* (5), 744–748.
- (10) Peng, K. Q.; Zhang, M. L.; Lu, A. J.; Wong, N. B.; Zhang, R. Q.; Lee, S. T. *Appl. Phys. Lett.* **2007**, *90* (16), No. 163123.
- (11) Zhang, M. L.; Peng, K. Q.; Fan, X.; Jie, J. S.; Zhang, R. Q.; Lee, S. T.; Wong, N. B. *J. Phys. Chem. C* **2008**, *112* (12), 4444–4450.
- (12) Hochbaum, A. I.; Fan, R.; He, R. R.; Yang, P. D. *Nano Lett.* **2005**, *5* (3), 457–460.
- (13) Kayes, B. M.; Filler, M. A.; Putnam, M. C.; Kelzenberg, M. D.; Lewis, N. S.; Atwater, H. A. *Appl. Phys. Lett.* **2007**, *91*, No. 103110.
- (14) Lu, Y.; Lal, A. *Nano Lett.* **2010**, *10* (11), 4651–4656.
- (15) Plass, K. E.; Filler, M. A.; Spurgeon, J. M.; Kayes, B. M.; Maldonado, S.; Bruntschwig, B. S.; Atwater, H. A.; Lewis, N. S. *Adv. Mater.* **2009**, *21* (3), 325–328.
- (16) Shiu, S. C.; Hung, S. C.; Chao, J. J.; Lin, C. F. *Appl. Surf. Sci.* **2009**, *255* (20), 8566–8570.
- (17) Li, X.; Bohn, P. W. *Appl. Phys. Lett.* **2000**, *77* (16), 2572–2574.
- (18) Bogush, G. H.; Tracy, M. A.; Zukoski, C. F. *J. Non-Cryst. Solids* **1988**, *104* (1), 95–106.
- (19) Hsu, C. M.; Connor, S. T.; Tang, M. X.; Cui, Y. *Appl. Phys. Lett.* **2008**, *93* (13), No. 133109.
- (20) Sinitiskii, A.; Neumeier, S.; Nelles, J.; Fischler, M.; Simon, U. *Nanotechnology* **2007**, *18* (30), No. 305307.
- (21) Peng, K. Q.; Lu, A. J.; Zhang, R. Q.; Lee, S. T. *Adv. Funct. Mater.* **2008**, *18* (19), 3026–3035.
- (22) Huang, Z. P.; Shimizu, T.; Senz, S.; Zhang, Z.; Zhang, X. X.; Lee, W.; Geyer, N.; Gosele, U. *Nano Lett.* **2009**, *9* (7), 2519–2525.
- (23) Huang, Z. P.; Shimizu, T.; Senz, S.; Zhang, Z.; Geyer, N.; Gosele, U. *J. Phys. Chem. C* **2010**, *114* (24), 10683–10690.
- (24) Lee, C. L.; Tsujino, K.; Kanda, Y.; Ikeda, S.; Matsumura, M. *J. Mater. Chem.* **2008**, *18* (9), 1015–1020.
- (25) Vitko, J.; Benner, R. E.; Shelby, J. E. *Sol. Energy Mater.* **1983**, *9* (1), 51–67.

- (26) Waters, P.; Volinsky, A. A. *Exp. Mech.* **2007**, *47* (1), 163–170.
- (27) Chartier, C.; Bastide, S.; Levy-Clement, C. *Electrochim. Acta* **2008**, *53* (17), 5509–5516.
- (28) Qu, Y. Q.; Liao, L.; Li, Y. J.; Zhang, H.; Huang, Y.; Duan, X. F. *Nano Lett.* **2009**, *9* (12), 4539–4543.
- (29) Douani, R.; Si-Larbi, K.; Hadjersi, T.; Megouda, N.; Manseri, A. *Phys. Status Solidi A* **2008**, *205* (2), 225–230.
- (30) Peng, K. Q.; Hu, J. J.; Yan, Y. J.; Wu, Y.; Fang, H.; Xu, Y.; Lee, S. T.; Zhu, J. *Adv. Funct. Mater.* **2006**, *16* (3), 387–394.
- (31) Peng, K. Q.; Fang, H.; Hu, J. J.; Wu, Y.; Zhu, J.; Yan, Y. J.; Lee, S. *Chem—Eur. J.* **2006**, *12* (30), 7942–7947.
- (32) Peng, K. Q.; Wu, Y.; Fang, H.; Zhong, X. Y.; Xu, Y.; Zhu, J. *Angew. Chem. Int. Ed.* **2005**, *44* (18), 2737–2742.
- (33) Kalem, S.; Werner, P.; Nilsson, B.; Talalaev, V. G.; Hagberg, M.; Arthursson, O.; Sodervall, U. *Nanotechnology* **2009**, *20*, 44.
- (34) Xie, P.; Hu, Y. J.; Fang, Y.; Huang, J. L.; Lieber, C. M. *Proc. Natl. Acad. Sci. U.S.A.* **2009**, *106* (36), 15254–15258.
- (35) Fan, Z. Y.; Ho, J. C.; Jacobson, Z. A.; Yerushalmi, R.; Alley, R. L.; Razavi, H.; Javey, A. *Nano Lett.* **2008**, *8* (1), 20–25.
- (36) Pevzner, A.; Engel, Y.; Elnathan, R.; Ducobni, T.; Ben-Ishai, M.; Reddy, K.; Shpaisman, N.; Tsukernik, A.; Oksman, M.; Patolsky, F. *Nano Lett.* **2010**, *10* (4), 1202–1208.
- (37) Jalabert, L.; Bottier, C.; Kumemura, M.; Fujita, H. *Microelectron. Eng.* **2010**, *87* (5–8), 1431–1434.
- (38) Xu, S.; Qin, Y.; Xu, C.; Wei, Y. G.; Yang, R. S.; Wang, Z. L. *Nat. Nanotechnol.* **2010**, *5* (5), 366–373.
- (39) Thangawng, A. L.; Ruoff, R. S.; Swartz, M. A.; Glucksberg, M. R. *Biomed. Microdevices* **2007**, *9* (4), 587–595.